Journal of the European Ceramic Society **16** (1996) 161–168

0955-2219(95)00145-X
0955-2219/96/$15.00

Germanium Mullite: Structure and Vibrational Spectra of Gels, Glasses and Ceramics

D. Michel,[a] Ph. Colomban,[b]* S. Abolhassani,[c†] F. Voyron[c] & A. Kahn-Harari[c]

[a]CECM, CNRS UPR 2801, 15 rue G. Urbain, 94407 Vitry, France
[b]LASIR, CNRS UPR 2631, 2 rue H. Dunant, 94320 Thiais, France
[c]ENSCP, URA CNRS 1466, 11 rue P. et M. Curie, 75005 Paris, France

(Accepted 22 July 1995)

Abstract

The Raman spectra of mullite phases in GeO_2–Al_2O_3 and GeO_2–Ga_2O_3 systems are compared with those of silicon mullite and sillimanite. Replacement of silicon by germanium and aluminium by gallium modifies the wavenumbers of certain lines, especially at high frequency. However, all germanium mullites present similar features which reflect their disordered character. Even for compositions Al_2GeO_5 and Ga_2GeO_5 which are homologous to that of sillimanite, Raman spectra consist of broad bands, as previously observed in silicon mullites. The evolution of spectra is discussed for a series of $Al_{4+2x}Ge_{2-2x}O_{10-x}$ mullite phases with $0 < x < 0{\cdot}47$. The spectra of amorphous gels and glasses prepared by slow hydrolysis–polycondensation of aluminium and germanium (silicon) alkoxide mixtures show rather narrow bands. This indicates that the polymeric arrangement of molecular entities is less distorted in non-crystalline precursors than in crystalline mullite. Finally, a phase relation diagram is proposed for the sol–gel route.

Introduction

Phases isostuctural with silicon mullites exist in the GeO_2–Al_2O_3 phase diagram.[1–5] However, whereas at atmospheric pressure mullite is the only aluminosilicate formed, two other stable compounds exist with germanium: Al_2GeO_5, isostructural with the high-pressure silicate kyanite,[4] and $Al_2Ge_2O_7$ in which Al atoms are in five-fold oxygen coordination.[6] In addition, the metastable phase Al_4GeO_8, isostructural to β-Ga_4GeO_8, can be obtained.[7]

*To whom correspondence should be addressed.
†Present address: Electron Microscopy Center, University of Lausanne, Bugnon 27, 1005 Lausanne, Switzerland.

As well as $Al_{4+2x}Si_{2-2x}O_{10-x}$ mullites,[8] Ge mullites have an extended stability range, but the domain of stability differs for germanates and silicates.[4,8,9] In particular, the Ge mullite range of composition includes Al_2GeO_5 ($x = 0$), which corresponds to that of high-pressure Al_2SiO_5 sillimanite.

An 'ideal' mullite structure ($x = 0$) can be described as a disordered variety of sillimanite in which aluminium and silicon atoms are randomly distributed on the tetrahedral sites.[10–12] On the contrary, in sillimanite, Al and Si atoms regularly alternate along the tetrahedral chains. This leads to a doubling of the c lattice constant and to a change in the space group from *Pbam* to *Pbnm* (*Pnma* in a standard setting after permutation of axes). In addition to the disorder on tetrahedral sites, $Al_{4+2x}Si(\text{or } Ge)_{2-2x}O_{10-x}$ mullites are non-stoichiometric phases with oxygen vacancies when $x \neq 0$. Structure refinements on Si or Ge mullites indicate that the vacancies affect a special set of oxygen positions usually labelled O_c and that the neighbouring cations occupy new sites (Tet*) in order to maintain a tetrahedral environment, as shown in Fig. 1.[9–14] Consequently, the local structure of mullite is very complex. In particular, various states of order have been observed on germanium mullites depending on composition and thermal treatments.[15–18]

The present work reports a Raman scattering study on Ge mullites in a large range of composition, $0 < x < 0{\cdot}47$ (from 50 to 70 mol% Al_2O_3). In addition, the spectrum of mullite Ga_2GeO_5 clarifies the effect of substitution of aluminium by gallium. Results on crystallized mullite ceramics obtained by high temperature processes are compared with those of monoliths prepared from a sol–gel route in order to understand structural changes in glass ceramics and poorly crystallized samples from modifications of their Raman spectra.

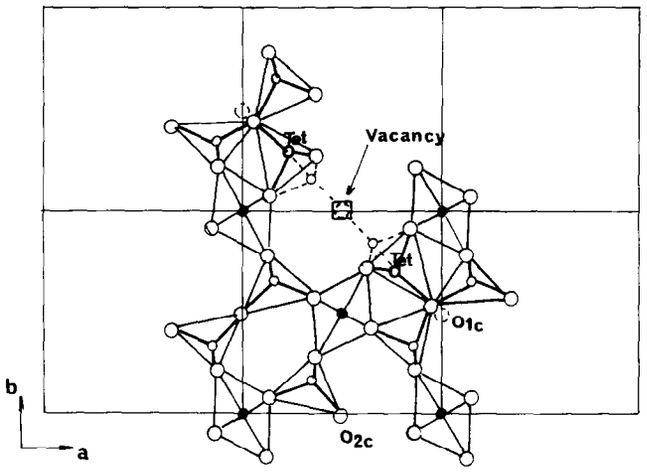

Fig. 1. Projection of the structure of mullite on (0 0 1) showing the environment of an oxygen vacancy on O_c positions and occupancy of new tetrahedral sites Tet*.

Experimental Procedure

Samples were prepared by two methods. The first method was used to obtain well-crystallized Al and Ga germanates giving the reference Raman spectra of the various phases. In this case, the synthesis route was coprecipitation with ammonia of mixed germanium oxide (quartz form soluble in hot water) and Al(or Ga)$(NO_3)_3 \cdot 9H_2O$ aqueous solutions. Atomic absorption analysis on the residual solutions verified that cation losses during the process are negligible. After dehydration, powders were pressed into pellets and heat-treated for 15 h at 1500°C in sealed platinum tubes to prevent GeO_2 volatilization. Then, samples were annealed for 30 h at 1330°C. The characterization of resulting phases and determination of their lattice constants were performed by X-ray diffraction and the results are reported elsewhere.[18] Raman spectra of these samples were recorded with a Jobin-Yvon Ramanor HG2S apparatus with a double monochromator using the blue (λ = 488·0 nm) or green (λ = 514.5 nm) lines of an Ar laser. The slit width was kept to about 1–2 cm^{-1}.

The second series of samples was obtained within the framework of studies on mullite formation and sintering using the sol–gel route.[19–23] In particular, the substitution of germanium to silicon strongly decreases the refractarity and helps to densify mullite composites.[24] Monolithic, optically clear gels were prepared by slow hydrolysis (several months) of mixed aluminium secondary butoxide and germanium ethoxide or silicon methoxide diluted in hexane (ratio alkoxide/hexane = 1/5 by volume). Due to the highly hygroscopic nature of the alkoxides, mixture preparation was performed under argon in a glove box free of water traces ($H_2O < 20$ ppm). Hydrolysis and evacuation of hexane and alcohols resulting from hydrolysis–polycondensation then proceeds in air through the polyethylene stopper of a glass flask as previously described.[21] The mixture becomes viscous, gels and, because of its volume contraction, separates from the flask. Heat treatments were then applied in air at various temperatures. Materials remain optically clear up to 1110–1200°C depending on composition. The crystallization process and phase transitions were followed by differential thermal analysis (DTA), dilatometry and X-ray diffraction. The composition and homogeneity were checked by EDX analysis. Hot-pressed pellets were also prepared using graphite dyes and resistors.

The Raman spectra of samples prepared from organic precursors were recorded with a XY Dilor multichannel spectrometer equipped with a Wright 1200-300 CCD detector cooled with nitrogen. Light was collected with an Olympus microscope at a magnification of 1000 ×. Laser excitation was made by the 514·5 nm argon line. Due to the very weak intensity of some spectra, artefacts coming from the collection optics appeared on some spectra around 550 and 1080 cm^{-1} (broad bands) and 842 and 916 cm^{-1} (narrow lines). These artefacts are labelled on Fig. 3

Results and Discussion

Relation between spectra of mullite and sillimanite

The Raman spectra of silicon mullites and alumina–silica glass obtained by fast quenching were studied by McMillan and Piriou.[25] A complete interpretation of the Raman spectra of sillimanite was made from the study of polarized spectra by Salje and Werneke[26] and the effect of pressure was discussed by Mernagh and Liu.[27] These results give a useful classification for the Raman modes and have been of considerable help for our interpretation of spectra of germanates with parent structures.

The irreducible representations corresponding to sillimanite are

$$\Gamma = 13\,A_g + 13\,B_{1g} + 8\,B_{2g} + 8\,B_{3g} + 11\,A_u + 11\,B_{1u} + 16\,B_{2u} + 16\,B_{3u}$$

including the acoustical modes

$$\Gamma_{\text{acoust.}} = B_{1u} + B_{2u} + B_{3u}$$

Therefore, there are 42 Raman active (13 Ag + 13 B_{1g} + 8 B_{2g} + 8 B_{3g}) and 40 infra-red active (10 B_{1u} + 15 B_{2u} + 15 B_{3u}) modes for sillimanite.

For an 'ideal' mullite with no oxygen vacancies (x = 0), the irreducible representations decompose as follows :

$$\Gamma = 6\,A_g + 6\,B_{1g} + 3\,B_{2g} + 3\,B_{3g} + 5\,A_u + 5\,B_{1u} + 10\,B_{2u} + 10\,B_{3u}$$

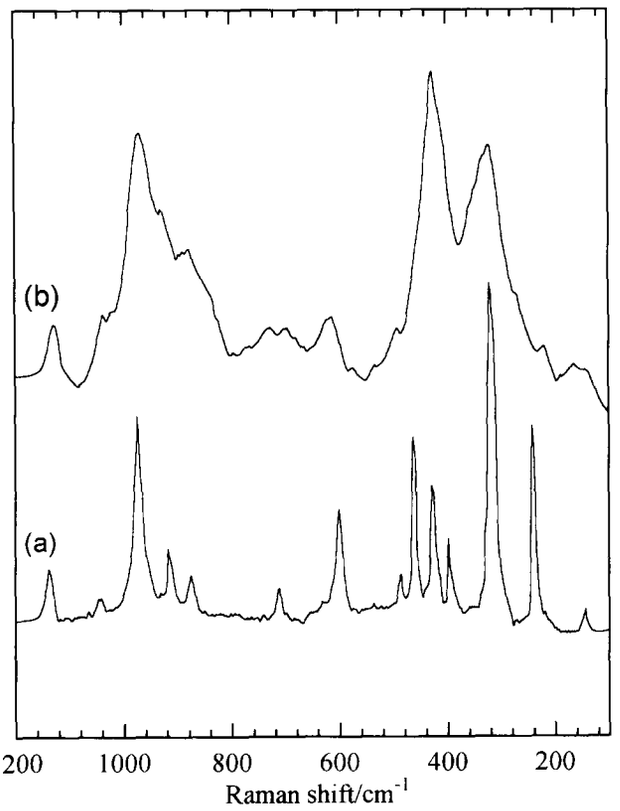

Fig. 2. Raman spectra of: (a) sillimanite from Pinet *et al.*;[30] (b) a 55 mol% Al_2O_3 mullite (x = 0·13) from McMillan and Piriou.[25]

including

$$\Gamma_{acoust.} = B_{1u} + B_{2u} + B_{3u}$$

There are 18 Raman (6 A_g + 6 B_{1g} + 3 B_{2g} + 3 B_{3g}) and 22 infra-red (4 B_{1u} + 9 B_{2u} + 9 B_{3u}) active modes.

It should be pointed out that in mullite and sillimanite the Al atoms in octahedral sites are on an inversion centre and do not participate in the Raman activity. Scattering coming from cations concerns only tetrahedral Al and Si(or Ge) atoms. For the same reason, the O_c atoms in mullite located at the common corner of two tetrahedra (2a Wyckoff positions) are not involved in the Raman spectra. By symmetry, all the Raman modes of a mullite with x = 0 directly derive from degeneracy of sillimanite Raman modes. In particular, mullite modes corresponding to metal and oxygen atoms in 4h Wyckoff positions are split into two for sillimanite. Atoms of type O_c are no longer on an inversion centre in sillimanite and six Raman active modes ($2A_g + 2B_{1g} + B_{2g} + B_{3g}$) are due to vibration of these atoms.

In mullite, the random occupancy of tetrahedral sites by Al and Si, as well as the presence of oxygen vacancies and of new tetrahedral sites when $x \neq 0$, induce breakdown of the translational symmetry of the crystal. In the case of mixed crystals and solid solutions containing a high content of such massive point defects, the selection rules do not apply and Raman spectra consists of broad bands which tend to reproduce the phonon density of states. A good example can be found in stabilized zirconias, the spectrum of which consists of a broad continuum.[28,29] Similar features have actually been observed on silicon mullites, as shown in the spectrum of a 55 mol% Al_2O_3 mullite obtained by McMillan and Piriou[25] given in Fig. 2(b). Figure 2(a) represents the spectrum of sillimanite obtained by Pinet *et al.*[30] Contrary to sillimanite which displays narrow and precisely defined lines, the mullite spectrum consists of broad lines, but each Raman band of mullite can be directly related to corresponding lines in sillimanite. This illustrates well the structural relation between mullite and sillimanite, which possess the same framework of octahedral and tetrahedral chains.

The spectra of Si mullites with compositions x = 0·25 and 0·5 prepared from the sol–gel route are given in Fig. 3 and results on mullite and sillimanite spectra are gathered in Table 1. Silicon

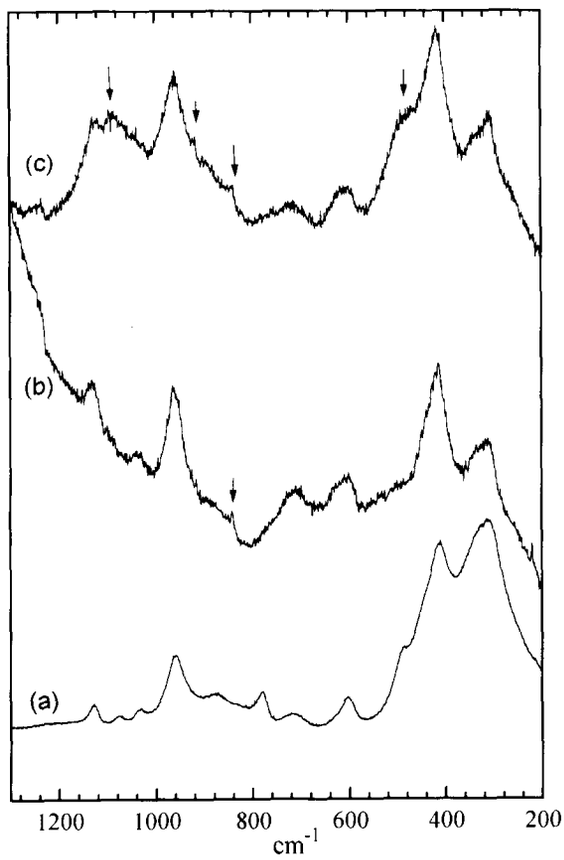

Fig. 3. Raman spectra of silicon mullites with various compositions prepared by a sol–gel route: (a) optically clear nanocrystalline glass-ceramic monolith after 4 days at 1100°C (composition Al_2O_3–$2SiO_2$); (b) pellet (x = 0·25, 60 mol% Al_2O_3) hot-pressed at 1600°C for 2 h (the broad band above 1200 cm^{-1} is due to graphitic precipitates); (c) pellet (x = 0·5, 71 mol% Al_2O_3) sintered at 1650°C for 3 h in air (arrows indicate the bands arising from the optics).

Table 1. Raman frequencies of sillimanite and Si-mullites

Sillimanite (Ref. 30)	*Al_2O_3–2SiO_2 glass-ceramic, sol–gel route, 1100°C*	*Mullite x = 0·25, sol–gel route, 1600°C*	*Mullite x = 0·5, sol–gel route, 1650°C*	*Mullite (Ref. 25)*
144 w				
236 s				
311 vs	310 vs	314 m	308 m	310 s
393 w				
413 w	413 m	415 s	416 s	410 s
423 m				
459 s				
485 w				
597 m	603 w	607 m	607 m	610 w
706 w	715 vw	711 m	718 w	710 w
849 vw	780 w			
874 w	873 w	873 w	875 sh	880 sh
910 w				
966 s	960 m	962 s	960 s	960 s
1036 w	1033 vw	1033 w		1040 m
1060 w	1077 vw	1080 w	1090 w	
1132 w	1129 w	1130 m	1125 w	1160 m

s: Strong; m: medium; w: weak; vw: very weak; sh: shoulder.

mullites, as well as silicon-containing glasses and gels, are generally poor Raman scatterers[19,20] and this explains the high noise level in the spectra of Figs 2(a), 3(b) and 3(c). However, the spectrum of the nanocrystalline glass-ceramic monolith (Fig. 3(a)) is better resolved. Local arrangements in the first steps of crystallization from gels seem to be less distorted and better defined than after high-temperature treatments.

Spectra of germanium mullites

The Raman spectra of germanium mullites with various compositions, prepared by coprecipitation and by the sol–gel route, are given in Figs 4 and 5, respectively. For the same composition, the Raman spectra of samples prepared by the two methods are very similar. This indicates that the evolution of Raman spectra with composition represents the intrinsic structural change. Corresponding wavenumbers are gathered in Table 2.

All these spectra are very similar to those of silicon mullites except for the wavenumbers, which are shifted towards low values for most lines. For all compositions, the spectra consist of broad lines as for Si mullite. The line width at half maximum amounts to about 40 cm^{-1}, which is more than twice than in sillimanite. In addition, broader bands with asymmetric profiles around 300 and 600 cm^{-1} are probably the envelope of two or more lines. For the Al_2GeO_5 compound where no oxygen vacancies are present ($x = 0$), these features can be only attributed to a disordered distribution of Al and Ge on tetrahedral sites. This confirms previous results obtained by infra-red spectroscopy[4,31] and by electron and X-ray diffraction patterns, as there is no diffraction spot or diffuse scattering indicating a double periodicity along the *c*-axis.[17]

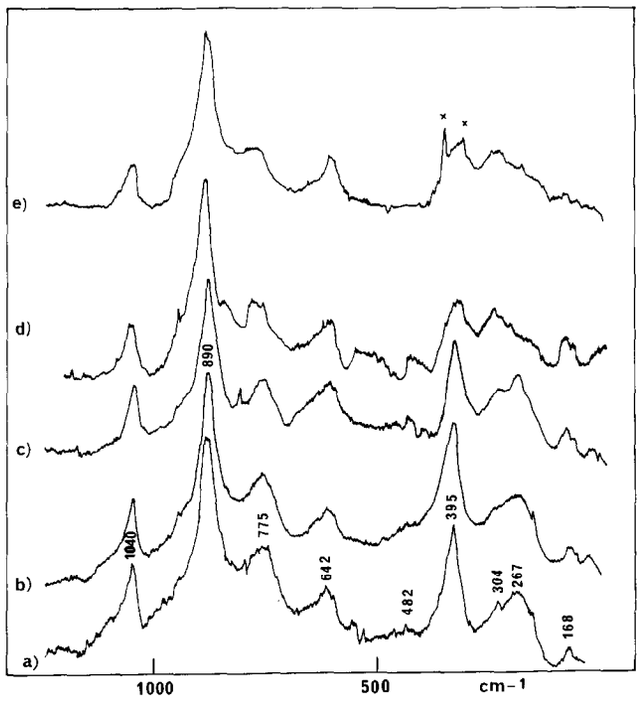

Fig. 4. Raman spectra of $Al_{4+2x}Si_{2-2x}O_{10-x}$ germanium mullites annealed at 1330°C: (a) $x = 0$ (50 mol% Al_2O_3); (b) $x = 0{\cdot}13$ (55 mol% Al_2O_3); (c) $x = 0{\cdot}25$ (60 mol% Al_2O_3); (d) $x = 0{\cdot}40$ (67 mol% Al_2O_3); (e) $x = 0{\cdot}47$ (70 mol% Al_2O_3). Traces of a Al_2O_3 are revealed by the lines at 380 and 417 cm^{-1} indicated by x.

The general aspect of the spectra remains essentially unchanged with composition for the series of

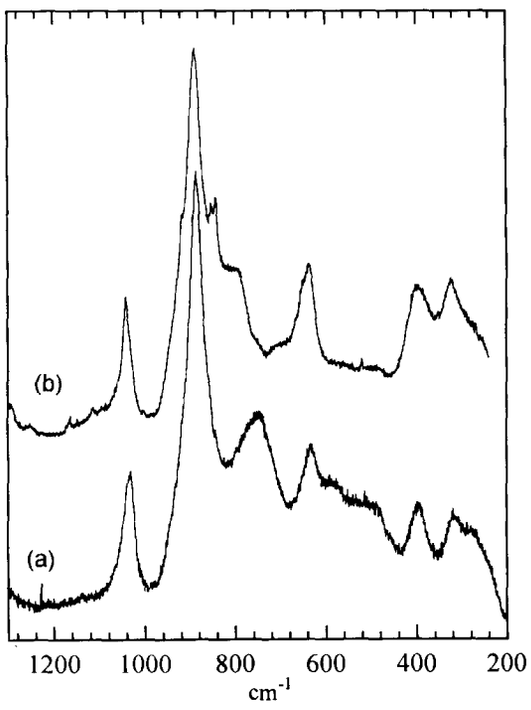

Fig. 5. Raman spectra of $Al_{4+2x}Ge_{2-2x}O_{10-x}$ germanium mullites prepared by sol–gel route: (a) optically clear monlith $x = 0{\cdot}15$ (56 mol% Al_2O_3) obtained after 3 h at 1000°C; (b) translucent monolith $x = 0{\cdot}25$ (60 mol% Al_2O_3) obtained at 1250°C.

Table 2. Raman frequencies of $Al_{4+2x}Ge_{2-2x}O_{10-x}$ germanium mullites as a function of composition (mol%). Samples prepared by sol–gel route are indicated by *

50% Al_2O_3 x = *0*, *1330°C*	*55% Al_2O_3* x = *0·13*, *1330°C*	*56% Al_2O_3* x = *0·15*, *1000°C**	*60% Al_2O_3* x = *0·25*, *1330°C*	*60% Al_2O_3* x = *0·25*, *1250°C**	*67% Al_2O_3* x = *0·40*, *1330°C*	*70% Al_2O_3* x = *0·47*, *1330°C*
170 w	165 w	[a]	170 w	[a]	170 w	170 w
265 m	270 m	270 w	250 m		260 m	260 m
305 m	305 sh	315 w	300 m	320 m	300 m	310 s
395 s	395 s	395 s	395 s	395 m	395 s	395 m
480 vw	480 vw	490 vw		480 vw	480 vw	
570 vw		580 vw	570 vw		570 vw	
640 m	640 m	635 m	640 m	635 m	640 m	640 m
775 m	780 m	790 m	785 m	790 m	785 m	795 m
890 vs	890 vs	890 vs	890 vs	890 vs	890 vs	890 w
945 sh	945 sh		945 sh		945 sh	950 sh
1040 m	1040 m	1040 m	1045 m	1040 m	1050 m	1055 sh

s: Strong; m: medium; w: weak; vw: very weak; sh: shoulder.
[a] Not studied below 200 cm^{-1}.

Fig. 4. However, modification occurs in the shape, intensity or position of certain bands. Wavenumbers are slightly shifted towards lower frequencies as the alumina content increases for two high frequency lines (from 1040 to 1055 cm^{-1} and from 775 to 795 cm^{-1}). On the other hand, the location of the 640 and 395 cm^{-1} lines does not vary, though the 395 cm^{-1} line decreases and broadens as the alumina content increases. Noticeable intensity changes are also observed for the 260 and 310 cm^{-1} lines depending on composition.

The Raman spectrum of a Ga_2GeO_5 mullite ($x = 0$) given in Fig. 6 has a close resemblance with that of Al_2GeO_5 despite a significant shift towards low frequency (about 50 cm^{-1}) for the bands in the region 700–1100 cm^{-1}. Another difference is the better resolution of the broad band between 200 and 350 cm^{-1} for the gallium compound. This result is in agreement with the observation by Schneider[31] of some band splitting in infra-red spectroscopy which was interpreted in terms of slight ordering.

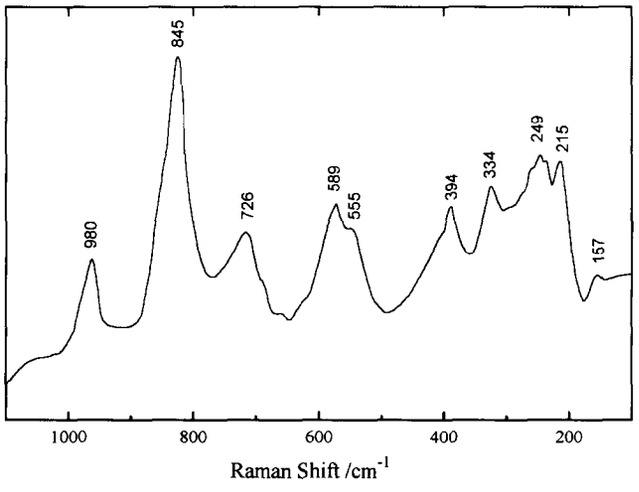

Fig. 6. Raman spectrum of Ga_2GeO_5 mullite.

The high frequency modes of Al(or Ga)$_2GeO_5$ mullites (1045, 950, 885 and 785 cm^{-1} with Al and 980, 845 and 726 cm^{-1} with Ga) correspond to the ν_1 and ν_3 internal modes of GeO_4 groups. These modes are found at much higher wavenumbers than for isolated GeO_4 groups. They appear, for instance, in the range 800–700 cm^{-1} in scheelite orthogermanates.[32] Salje and Werneke suggested that the coupling with neighbouring Al–O bonds explains the increased frequencies of SiO_4 stretching vibrations in andalusite and sillimanite.[26] The frequency difference in Ga and Al compounds that we observed probably results from the weaker Ga–O stretching force constants and the larger unit-cell parameters in Ga_2GeO_5. In silicon mullites, the corresponding modes are found at higher frequencies, respectively at 1140, 1040, 960 and 880 cm^{-1},[25] in good agreement with the difference usually observed between Ge–O and Si–O stretching.[33]

The asymmetric band at 640 cm^{-1} in Al–Ge mullite may be assigned to Al–O vibrations and those at 555 and 589 cm^{-1} in Ga_2GeO_5 to Ga–O vibrations. Actually, they are located in the same mid-wavenumber region where McMillan and Piriou have suggested to attribute Al–O displacement in mullite.[25] Moreover, Mernagh and Liu found lower Gruneisen parameters for the 708 and 594 cm^{-1} sillimanite modes which is indicative of more ionic bonding and may correspond to Al–O vibrations.[27]

A relatively well-defined line appears at 395 cm^{-1} in Al_2GeO_5 ($x = 0$) in the region corresponding to O–Ge–O bending in orthogermanates.[32] This line is severely affected when the alumina content increases and this is attributed to the decrease of the number of GeO_4 tetrahedra at the expense of AlO_4 units. Moreover, a similar line is found in Ga_2GeO_5 practically at the same frequency whereas in silicon mullite this band is at 410 cm^{-1}.

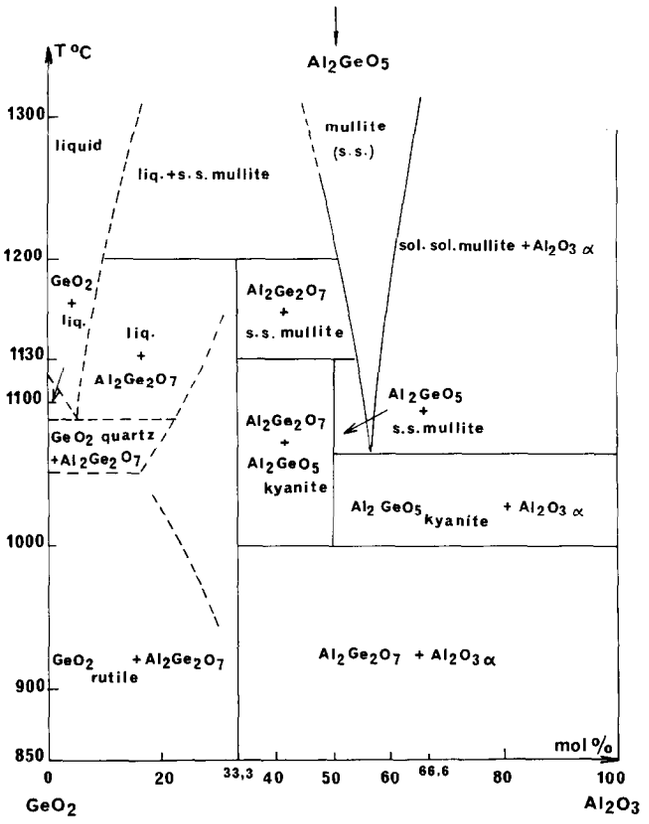

Fig. 7. GeO_2–Al_2O_3 phase diagram, after Perez y Jorba.[4]

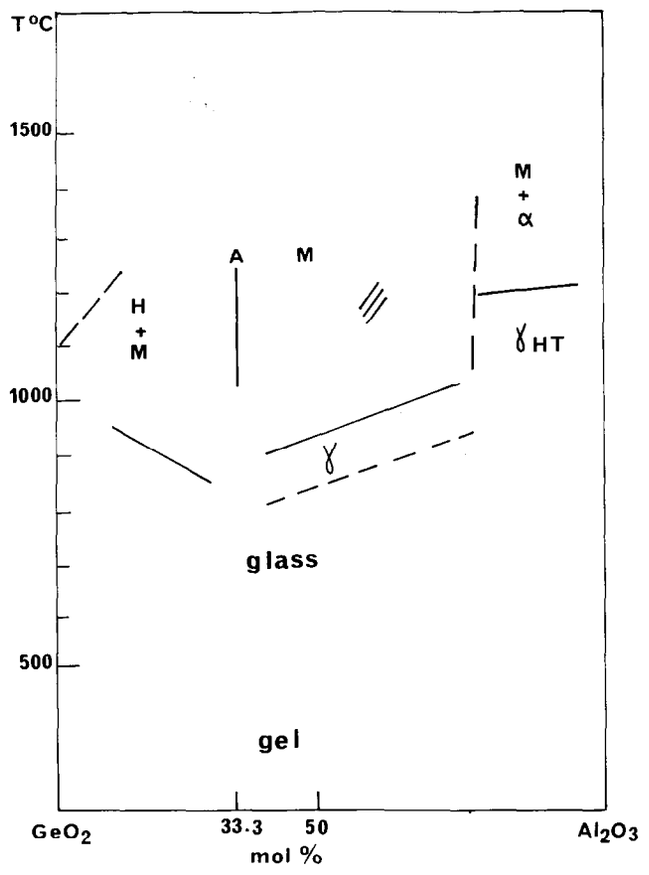

Fig. 8. Phase boundaries observed for gels prepared by slow alkoxide hydrolysis as a function of the composition and thermal treament (H = hexagonal GeO_2 (quartz-form), M = mullite, α = Al_2O_3 (corundum), γ = disordered phase exhibiting a spinel-like X-ray diffraction pattern, γ_{HT} = spinel phase, A = monoclinic $Al_2Ge_2O_7$, /// = metastable Al_4GeO_8).

The new local arrangements formed as the alumina content increases, in particular the groups of three tetrahedra linked by the same corner (Fig. 1), are expected to modify the Raman activity concerning collective vibrations. The observed change in the shape and intensity of bands with the Al/Ge ratio in the region below 380 cm^{-1}, which corresponds to external rotational and translational modes, is probably associated with these modifications.

Mullite formation and GeO_2–Al_2O_3 phase diagram

GeO_2–Al_2O_3 phase diagrams established by the study of materials prepared solely by solid-state reaction lead to a rather simple diagram, including mullite as the only binary compound similarly to that of SiO_2–Al_2O_3.[2,5] On the contrary, when the composition–temperature range is precisely explored using reactive powders, a more complex phase diagram is achieved (Fig. 7). Similarly, the crystal-

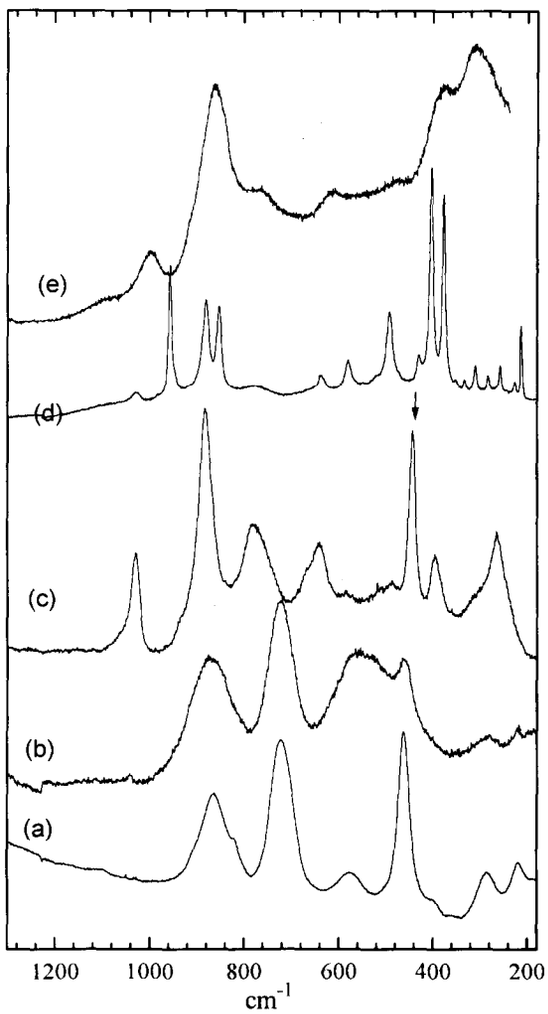

Fig. 9. Evolution of Raman spectra for the composition 2 GeO_2–Al_2O_3 (33·3 mol% Al_2O_3) depending on temperature: (a) water-containing gel (room temperature); (b) mesoporous glass obtained after heating at 800°C; (c) crystallized mullite + hexagonal GeO_2 (indicated by arrow) obtained after heating at 1020°C; (d) monoclinic $Al_2Ge_2O_7$ obtained after heating for 30 min at 1250°C; (e) high temperature mullite obtained after heating for 3 min at 1450°C.

lization of homogeneous gels leads to a variety of stable or metastable phases. Figure 8 summarizes the results obtained by annealing optically clear Al_2O_3–GeO_2 gels and gives the domains where the various phases are formed depending on temperature and the Al/Ge ratio. An example of successive structural changes is shown by Fig. 9, which reports the Raman spectra obtained after heating Al_2O_3–$2GeO_{2-x}H_2O$ gels at various temperatures. Corresponding wavenumbers are given in Table 3. In the gel state, the Raman spectrum consists of well-defined bands (Fig 9(a)) that can be assigned to the vibrations of GeO_4 (460 and 565 cm^{-1}) and GeO_6 (720 and 870 cm^{-1}) entities because this spectrum looks like the superimposition of quartz (443 and 880 cm^{-1}) and rutile (695 and 870 cm^{-1}) germania. Dehydration of this gel leads to a mesoporous glass which possesses the same Raman lines, but which are noticeably broadened. In addition, a very broad band which is characteristic of GeO_2 glass[34] is observed around 570 cm^{-1} (Fig. 9(b)). At higher temperature, crystallized phases are obtained, the first of which is mullite with some GeO_2 (quartz form). The Raman lines of this mullite phase (Fig. 9(c)) are relatively well defined. Mullite and GeO_2 quartz then transform into the monoclinic $Al_2Ge_2O_7$ compound. Its Raman spectrum (Fig. 9(d) contains only very sharp lines in agreement with X-ray results on single crystals which indicated that the structure of $Al_2Ge_2O_7$ is completely ordered.[6] The polyhedra present in this compound are Ge_2O_7 groups consisting of two tetrahedra linked by one corner and AlO_5 bipyramids.[6] According to the phase diagram given in Fig. 7, $Al_2Ge_2O_7$ is the phase stable below 1200°C; however, crystallization of gels leads first to mullite rather than directly into $Al_2Ge_2O_7$. It is likely that the preparation from hydrolysis–polycondensation favours a connected tetrahedra network and induces crystallization into mullite that contains similar arrangments. At higher temperature, the stable phase mullite appears again, but the significant line width of Raman bands reveals a large amount of disorder (Fig. 9(e)).

Table 3. Raman frequencies of the spectra of Fig. 9. Samples prepared by sol–gel route at the comparision 2 GeO_2–Al_2O_3 (33·3 mol% Al_2O_3)

Gel, 20°C	*Glass, 800°C*	*Mullite + GeO_2, 1020°C*	*$Al_2Ge_2O_7$, 1250°C*	*Mullite, 1450°C*
			214 m	
220 m	220 vw		228 vw	
		265 m	256 w	
285 m	283 w		284 w	
		312 m	311 w	300 m,b
			334 vw	
			352 vw	
			378 s	
400 vw	400 v w		403 s	390 s,b
		443 s	430 w	
462 s	461 m			
		487 w	492 m	
575 m	570 s,b		591 w	600 m,b
		641 m	638 w	
		670 sh		
722 s	723 s			
780 m,b		780 m	776 w,b	780 m,b
823 sh				
			854 s	
864 s	869 m,b			
		883 s	881 m	890 s,b
			957 m	
		1030 m	1030 w	1030 m,b

s: Strong; m: medium; w: weak; vw: very weak; sh: shoulder; b: broad.

Conclusions

Raman scattering studies demonstrated that both silicon and germanium mullites are strongly disordered at the molecular scale. In the case of the GeO_2–Al_2O_3 system, in addition to mullites with various degrees of order, (which can be estimated from Raman line width), several phases can be prepared with methods which favour mixing at molecular scale: $Al_2Ge_2O_7$, Al_2GeO_5 (kyanite form), Al_4GeO_8 and spinel-like phases. Furthermore, the lower melting point of GeO_2 enhances the achievement of the stable state at lower temperature than in silicon-containing homologues.

Acknowledgements

The authors are indebted to Drs B. Piriou (CNRS, Ecole Centrale, Chatenay-Malabry) and B. Lasnier (University of Nantes) for helpful discussion and for kindly communicating their results on Raman spectra of silicon mullite and sillimanite.

References

1. Perez y Jorba, M., Tarte, P. & Collongues, R., Structure and properties of alumina–germanium dioxide compounds. *C.R. Acad. Sci.*, **257** (1963) 3417–20.
2. Miller, J. L. Jr., McCormick, G. R. & Ampian, S. G., Phase equilibria in the system GeO_2–Al_2O_3. *J. Am. Ceram. Soc.*, **50** (1967) 268–9.
3. Perez y Jorba, M., GeO_2–Al_2O_3 and GeO_2–Fe_2O_3 systems. Comparison with the silica corresponding systems. *Silicates Industriels*, **1** (1968) 11–7.
4. Perez y Jorba, M., Study of phases between germanium dioxide and some oxides of trivalent elements. *Rev. Int. Hautes Temp. et Refract.*, **6** (1969) 283–98.
5. Prochazka, S., Sintering and properties of dense aluminum germanates, In *Ceramics Powders*, ed. P. Vincenzini, Elsevier, Amsterdam, 1983, pp. 861–70.
6. Agafonov, V., Kahn, A., Michel, D. & Perez y Jorba, M., Crystal structure of a new digermanate $Al_2Ge_2O_7$. *J. Solid State Chem.*, **62** (1986) 402–4.

7. Kahn, A., Agafonov, V., Michel, D. & Perez y Jorba, M., New gallium germanates with tunnel structures: α-Ga_4GeO_8 and $Ga_4Ge_3O_{12}$. *J. Solid State Chem.*, **65** (1986) 377–82.
8. Cameron, W. E., Mullite: a substituted alumina. *Am. Mineral.*, **62** (1977) 747–55.
9. Michel, D., Abolhassani, S., Kahn, A., Agafonov, V. & Perez y Jorba, M., Aluminum, gallium and iron (*III*) germanates with aluminum silicate structures. In *Mullite and Mullite Matrix Composites*, Ceramic Transactions, Vol. 6, eds S. Somiya, R. F. Davies & J. A. Pask, The American Ceramic Society, Westerville, OH, 1990, pp. 159–66.
10. Burnham, C. W., Crystal structure of mullite. *Carnegie Inst. Washington Yearbk*, **63** (1964) 223–7.
11. Burnham, C. W., Composition limits of mullite and the sillimanite–mullite solid solution problem. *Carnegie Inst. Washington Yearbk*, **63** (1964) 227–8.
12. Durovic, S., Isomorphism between sillimanite and mullite. *J. Am. Ceram. Soc.*, **45** (1962) 157–61.
13. Durovic, S. & Fedji, P., Synthesis and crystal structure of germanium mullite and crystallographic parameters of D-mullites. *Silikaty*, **20** (1976) 97–112.
14. Angel, R. J. & Prewitt, C. T., Crystal structure of mullite: a re-examination of the average structure. *Am. Mineral.*, **71** (1986) 1476–82.
15. Saalfeld, H. & Guse, W., Mullite single crystal growth and characterization. In *Mullite and Mullite Matrix Composites*, Ceramic Transactions, Vol. 6, eds S. Somiya, R. F. Davies & J. A. Pask, The American Ceramic Society, Westerville, OH, 1990, pp. 73–101.
16. Perez-Ramirez, J. G., Michel, D. & Portier, J. R., Enhancing of small isolated domains and superstructures in high resolution of oxides. *Mater. Res. Soc. Proc.*, **139** (1989) 321–6.
17. Kahn-Harari, A., Abolhassani, S., Perez-Ramirez, J. G., Michel, D., Mazerolles, L., Portier, R. & Perez-Ramirez, J. G., Observation of ordering in silicon and germanium mullites. *J. Solid State Chem.*, **90** (1991) 234–48.
18. Abolhassani, S., Contribution to the study of mullite-type aluminum germanates. Thesis, University of Paris-Sud, 1991.
19. Colomban, Ph., Structure of oxide gels and glasses by IR and Raman scattering. II, mullites. *J. Mater. Sci.*, **24** (1989) 3011–20.
20. Colomban, Ph., Gel–glass–mullite transition and microstructure as a function of powder preparation, Stoichiometry and Zr(Ti) addition. In *Ceramic Powder Processing Science*, eds H. Hausner, E. R. Fuller & G. D. Messing, The American Ceramic Society, Westerville, OH, 1989, pp. 85–92.
21. Colomban, Ph. & Mazerolles, L., Nanocomposites in mullite–ZrO_2 and mullite–TiO_2 systems synthesized through hydrolysis gel routes. Microstructure and fractography. *J. Mater. Sci.*, **26** (1991) 3503–10.
22. Colomban, Ph., Jones, D. J., Grandjean, D. & Flank, A. M., EXAFS and XANES study of (Si, Ge) mullites gels and glasses prepared by slow hydrolysis of alkoxides. *J. Non-Cryst. Solids*, **147–148**, (1992) 135–40.
23. Colomban, Ph. & Vendange, V., Sintering of alumina and mullites prepared by slow hydrolysis of alkoxides: the role of the protonic species and pore topology. *J. Non-Cryst. Solids*, **147–148**, (1992) 245–50.
24. Colomban, Ph., Lagrange, J. L., Bruneton, E. & Mouchon, E., Sol–gel mullite matrix–SiC 2D woven fabrics composites with and without zirconia interphase. *J. Eur. Ceram. Soc.*, in press.
25. McMillan, P. & Piriou, B., The structures and vibrational spectra of crystals and glasses in the silica–alumina system. *J. Non-Cryst. Solids*, **53** (1982) 279–98.
26. Salje, E. & Werneke, C., The phase equilibrium between sillimanite and andalusite as determined from lattice vibrations. *Contrib. Miner. Petrol.*, **79** (1982) 56–67.
27. Mernagh, T. & Liu, L. G., Raman spectra from the Al_2SiO_5 polymorphs at high pressure and room temperature. *Phys. Chem. Minerals*, **18** (1991) 126–30.
28. Keramidas, V. G. & White, W. B., Raman scattering from $Ca_xZr_{1-x}O_{2-x}$, a system with massive point defects. *J. Chem. Phys.*, **34** (1973) 1873–8.
29. Michel, D., Perez y Jorba, M. & Collongues, R., Study by Raman spectroscopy of order–disorder phenomena occurring in some binary oxides with fluorite-related structures. *J. Raman Spectrosc.*, **5** (1976) 163.
30. Pinet, M., Smith, D. C. & Lasnier, B., Raman microprobe in gemmology. *Revue de Gemmologie*, (June 1992) 11–60.
31. Schneider, H., Infrared spectroscopic investigation of andalusite and mullite-type structures in the Al_2GeO_5–Fe_2GeO_5 and Al_2GeO_5–Ga_2GeO_5 systems. *N. Jb. Miner. Abh.*, **142** (1981) 11–123.
32. Vandenborre, M. T., Michel, D. & Ennaciri, A., Vibrational spectra and force fields of scheelite-type germanates. *Spectrochim. Acta.*, **45A** (1989) 721–7.
33. Lazarev, A. I., Mirgorodskii, A. P. & Ignatiev, *Vibrational Spectra of Complex Oxides: Silicates and Analogs*, Nauka, Leningrad, 1975.
34. Henderson, G. S., Bancroft, G. M., Fleet, M. E. & Rogers D. J., Raman spectra of gallium and germanium substituted silicate glasses: variation in intermediate order, *Am. Mineral.*, **70** (1985) 946–60.